THE JOURNAL OF BIOLOGICAL CHEMISTRY VOL. 281, NO. 33, pp. 23471–23481, August 18, 2006

The Proprotein Convertase SKI-1/S1P

*IN VITRO ANALYSIS OF LASSA VIRUS GLYCOPROTEIN-DERIVED SUBSTRATES AND EX VIVO VALIDATION OF IRREVERSIBLE PEPTIDE INHIBITORS**

Received for publication, December 22, 2005, and in revised form, June 19, 2006 Published, JBC Papers in Press, June 21, 2006, DOI 10.1074/jbc.M513675200

Antonella Pasquato[‡§], Philomena Pullikotil[‡], Marie-Claude Asselin[‡], Manuela Vacatello[¶], Livio Paolillo[¶], Francesca Ghezzo[§], Federica Basso[§], Carlo Di Bello[§], Monica Dettin[§], and Nabil G. Seidah[‡1]

From the [‡]Laboratory of Biochemical Neuroendocrinology, Clinical Research Institute of Montreal, Montreal, Quebec H2W 1R7, Canada , the [§]Department of Chemical Process Engineering, University of Padova, 35131 Padova, Italy, and the [¶]Department of Chemistry, University of Naples "Federico II", Complesso Universitario di Monte S. Angelo, 80126 Naples, Italy

Herein we designed, synthesized, tested, and validated fluorogenic methylcoumarinamide (MCA) and chloromethylketone-peptides spanning the Lassa virus GPC cleavage site as substrates and inhibitors for the proprotein convertase SKI-1/S1P. The 7-mer MCA (YISRRLL-MCA) and 8-mer MCA (IYISRRLL-MCA) are very efficiently cleaved with respect to both the 6-mer MCA (ISRRLL-MCA) and point mutated fluorogenic analogues, except for the 7-mer mutant Y253F. The importance of the P7 phenylic residue was confirmed by digestions of two 16-mer non-fluorogenic peptidyl substrates that differ by a single point mutation (Y253A). Because NMR analysis of these 16-mer peptides did not reveal significant structural differences at recognition motif RRLL, the P7 Tyr residue is likely important in establishing key interactions within the catalytic pocket of SKI-1. Based on these data, we established through analysis of pro-ATF6 and pro-SREBP-2 cellular processing that decanoylated chloromethylketone 7-mer, 6-mer, and 4-mer peptides containing the core RRLL sequence are irreversible and potent *ex vivo* SKI-1 inhibitors. Although caution must be exercised in using these inhibitors in *in vitro* reactions, as they can also inhibit the basic amino acid-specific convertase furin, within cells and when used at concentrations ≤100 μM these inhibitors are relatively specific for inhibition of SKI-1 processing events, as opposed to those performed by furin-like convertases.

With the advent of the genome sequencing, it became apparent that hydrolases represent ~4% of the total human/mouse genome, with an estimated 500–550 members comprised within the 5 classes of proteases (1). Whereas these proteases cleave their substrates either intra- or extracellularly, some of them are implicated in the limited proteolysis of secretory precursors. Among those, the 9 known proprotein convertases (PCs)[2] are members of a unique family of mammalian serine proteinases related to bacterial subtilisin (2–4). The PCs are responsible for the tissue-specific limited proteolysis of multiple polypeptide precursors, generating a large diversity of bioactive molecules in an exquisitely regulated manner. Whereas seven PCs (PC1/3, PC2, furin, PC4, PC5/6, PACE4, and PC7) cleave secretory precursors within the motif R-X_n-R↓, where $n = 0$, 2, 4, or 6, and X is a variable amino acid, except Cys, the other two convertases (SKI-1/S1P and NARC-1/PCSK9) cleave within the motifs R-X-(hydrophobic)-X↓ (3, 5–8) and VFAQ↓ (9), respectively.

Subtilisin-kexin-isozyme-1, known as SKI-1 (6, 10), is synthesized as an inactive precursor that is autocatalytically cleaved in the endoplasmic reticulum (ER) at two alternate B′ and B sites: RKVF^{133}↓ and RKVFRSLK^{137}↓, respectively. The latter products are then transported to the *cis*/*medial* Golgi whereupon they are further autocatalytically processed into a C-form at RRLL^{186}↓ (Fig. 1), generating the active SKI-1 enzyme devoid of its prosegment (5, 6, 8, 10). SKI-1 was simultaneously discovered by our group (10) and Goldstein and Brown (11) who called it site 1 protease (S1P), a key enzyme in the regulation of lipid metabolism and cholesterol homeostasis that cleaves the transcription factors sterol regulatory element binding proteins (SREBP-1 and SREBP-2) (11, 12). The latter are synthesized as precursors harboring two transmembrane domains separated by a short ER luminal loop and comprising N- and C-terminal cytosolic domains. These precursors are cleaved in an SREBP-cleavage-activating protein (SCAP)- and insulin-induced gene (INSIG)-dependent fashion. When cellular cholesterol levels are high, INSIG binds and retains the SCAP-SREBP complex in the ER. When cells are deprived of sterols, INSIG separates, allowing the transport of the SREBP-SCAP complex to the Golgi (12–14). Therein, a two-step proteolytic process (SKI-1 and site 2 protease S2P) (14) releases the

* This work was supported by Canadian Institutes of Health Research Grant MOP-36496 and a private donation from the Strauss Foundation. The costs of publication of this article were defrayed in part by the payment of page charges. This article must therefore be hereby marked "*advertisement*" in accordance with 18 U.S.C. Section 1734 solely to indicate this fact.

[1] To whom correspondence should be addressed: 110 Pine Ave., West Montreal, QC H2W 1R7, Canada. Tel.: 514-987-5609; Fax: 514-987-5542; E-mail: seidahn@ircm.qc.ca.

[2] The abbreviations used are: PC, proprotein convertase; AMC, 7-amino-4-methylcoumarin; cmk, chloromethylketone; dec, decanoyl; SKI-1, subtilisin kexin isozyme-1; S1P, site-1-protease; CHO, Chinese hamster ovary; WT, wild type; SREBP, sterol regulatory element-binding protein; nSREBP, nuclear sterol regulatory element-binding protein; ATF6, activating transcription factor 6; nATF6, nuclear activating transcription factor 6; RP-HPLC, reverse phase-high performance liquid chromatography; GPC, glycoprotein C of Lassa virus; MES, 2-morpholinoethanesulfonic acid; ER, endoplasmic reticulum; SCAP, SREBP-cleavage-activating protein; CREB, cAMP-response element-binding protein; LCMV, lymphocytic choriomeningitis virus; CCHFV, Crimean Congo hemorrhagic fever virus; MCA, methylcoumarinamide; LAV, Lassa virus; Fmoc, N^{α}-fluorenylmethoxycarbonyl; PDGF, platelet-derived growth factor; DMF, dimethylformamide; ESI-MS, electrospray ionization-mass spectrometry; TFE, trifluoroethanol; NOESY, nuclear Overhauser effect spectroscopy; NOE, nuclear Overhauser effect.

cytosolic N-terminal segments of SREBPs from cell membranes, allowing their translocation to the nucleus (nSREBP), where they activate transcription of more than 35 mRNAs coding for proteins/enzymes required for the biosynthesis and uptake of cholesterol and unsaturated fatty acids (15).

Similar to SREBPs, the ER-anchored type II membrane bound transcription factor ATF6 plays a major role in the unfolded protein response (16). Under normal conditions, it is held in the ER by the chaperone BIP, with its N-terminal DNA binding domain facing the cytosol and its COOH terminus in the ER lumen (17). Accumulation of improperly folded proteins in the ER, which can be induced by calcium depletion (thapsigargin) or inhibition of *N*-glycosylation (tunicamycin), leads to an ER-stress response resulting in BIP dissociation from pro-ATF6. The latter is then translocated in a SCAP-independent fashion to the Golgi where it is first cleaved by SKI-1 and then by S2P. This releases the cytosolic N-terminal domain, which reaches the nucleus (nATF6) to activate ER stress target genes (18, 19).

Other type II membrane-bound substrates (Fig. 1) include the basic leucine zipper transcription factor Luman, the cellular counterpart of herpes simplex virus VP16 (20), and the CREB-like proteins (21). Brain-derived neurotrophic factor is a soluble substrate and the study of its processing led to the initial cloning of SKI-1 (10). Recently, the soluble prosomatostatin was also shown to be cleaved by SKI-1 to release the N-terminal peptide antrin (22). Finally, SKI-1 was shown to play a major role in cartilage development in zebrafish (23) and in the processing of surface glycoproteins of infectious viruses such as Lassa (LAV) (24, 25), lymphocytic choriomeningitis (LCMV) (26, 27), and Crimean Congo hemorrhagic fever (CCHFV) (28) viruses (Fig. 1). In particular, Lassa fever is endemic in West Africa and is estimated to affect some 100,000 people annually. No vaccines or antivirals are available against these deadly viruses.

PC activities are routinely assayed using two types of fluorogenic substrates, peptidyl methyl coumarinamides (MCA) (29) and intramolecularly quenched fluorogenic peptides (5, 25, 30, 31). Processing at the peptide↓MCA bond causes a fluorescence wavelength shift allowing the detection of the released fluorescent AMC group. Intramolecularly quenched fluorogenic peptides contain an N-terminal fluorescent group *o*-aminobenzoic acid and a C-terminal quench fluorescence moiety 3-nitrotyrosine. Cleavage of intramolecularly quenched fluorogenic peptides releases the quenching effect and the released N-terminal *o*-aminobenzoic acid containing fragment is now free to fluoresce. Recently, we designed a 16-mer intramolecularly quenched fluorogenic substrate based on the processing site of GPC SKI-1 in Lassa (24), namely *o*-aminobenzoic acid-DIYISRRLL↓GTFTW-3-nitrotyrosine-A-amide, which turned out to be the best *in vitro* SKI-1 substrate known so far (25). In the present work, we designed and analyzed the kinetic properties of a number of MCA peptides based on viral glycoprotein recognition motifs as potential *in vitro* substrates for SKI-1 (Fig. 1).

The critical implication of SKI-1 in various cellular functions and in certain pathologies emphasizes the importance of developing specific inhibitors that modulate its activity in disease states. Whereas SKI-1 inhibition was recently achieved by 300 μM of the general serine protease inhibitor 4-(2-aminoethyl)benzenesulfonyl fluoride (32), the latter is not a specific SKI-1 inhibitor. We recently introduced protein-based *ex vivo* inhibitors of SKI-1 by mutagenizing the reactive site loop of α_1-antitrypsin. We also optimized the prosegment-based inhibition of SKI-1 and identified a unique R134E mutant exhibiting a potent inhibitory activity (33). In this work we developed small molecule-specific inhibitors of cellular SKI-1 *ex vivo* activity based on the best *in vitro* Lassa glycoprotein GPC cleavage site, coupled to an N-terminal decanoyl membrane permeable moiety and a C-terminal chloromethylketone irreversible inhibitor functionality. These could serve as first lead compounds for further refinement.

EXPERIMENTAL PROCEDURES

Synthesis of Viral Glycoprotein-derived MCA and Cmk Peptides—All fluorogenic peptides were synthesized in house, except for succinyl-RRLL-7-amido-4-MCA (GenScript Corp., Piscataway, NJ). Fluorogenic peptides derived from various viral glycoproteins, including LCMV (Armstrong and WE), MCA-GP$^{259-265}$, and CCHV MCA-GP$^{518-524}$ were synthesized in a similar fashion to Lassa virus (LAV) GPCs. The latter included MCA-GPC$^{252-259}$ (8-mer WT), MCA-GPC$^{253-259}$ (7-mer WT), MCA-GPC$^{254-259}$ (6-mer WT) and MCA-(Y253A,Y253S,Y253I,Y253F,Y253V)-GPC$^{253-259}$ (7-mer (Ala), 7-mer (Ser), 7-mer (Ile), 7-mer (Phe), 7-mer (Val)) (Fig. 3*B*). The synthesis without the C-terminal amino acid was achieved by SPPS (solid-phase methods) on a semi-automated Applied Biosystems model 431A synthesizer, using standard N^{α}-fluorenylmethoxycarbonyl (Fmoc) protocols and 2-(1*H*-benzotriazol-1-yl)-1,1,3,3-tetramethyluronium hexafluorophosphate/*N*-hydroxybenzotriazole as a coupling method on Fmoc-Leu-SASRIN resin (0.77 mmol/g, 0.25 mmol, Bachem, Bubendorf, Switzerland). The introduction of a decanoyl (dec, CH_3-$(CH_2)_9$-) group to the N terminus of the inhibitors was obtained by incubating the growing chain still anchored to the solid support with 4 equivalents (eq) of decanoic acid, 4 eq 2-(1*H*-benzotriazol-1-yl)-1,1,3,3-tetramethyluronium hexafluorophosphate/*N*-hydroxybenzotriazole, and 0.1 eq of 4-dimethylaminopyridine in dimethylformamide (DMF). The percentage of decanoylation was evaluated to be 100% by a Kaiser test. The C terminus of αN- and side chain-protected crude peptides was coupled to H-Leu-MCA (2 eq, Bachem, Bubendorf, Switzerland) or H-Leu-chloromethylketone (H-Leu-cmk) (2 eq, Bachem, Bubendorf, Switzerland) with 0.45 M (1 eq) 2-(7-aza-1*H*-benzotriazole-1-yl)-1,1,3,3-tetramethyluronium hexafluorophosphate/1-hydroxy-7-azabenzotriazole (HATU/HAOt) and 0.1 M 4-dimethylaminopyridine (0.1 eq) in DMF. For the fluorogenic peptides, after Fmoc removal (10% diisopropylethylamine in DMF), the succinyl group was introduced by succinic anhydride (10 eq) in DMF plus 0.1 M 4-dimethylaminopyridine to adjust the pH between 7 and 8. Final crude peptides were obtained after removal of side chain protecting groups by incubation in 10 ml of a mixture of 95% trifluroacetic acid, 2.5% H_2O, and 2.5% triethylsilane for 90 min. Each reaction step was monitored by reverse phase-high performance liq-

uid chromatography (RP-HPLC). After lyophilization, the crude fluorogenic products were purified by RP-HPLC on an analytical Vydac C_{18} column (5 μm, 300 Å, 4.6 × 250 mm), monitoring the elution (1 ml/min) at 214 nm and using as eluents, 0.05% trifluroacetic acid/H_2O (A), and 0.05% trifluroacetic acid/CH_3CN (B). The peptides were assayed for purity (>97%) by analytical HPLC and their identity confirmed by electrospray ionization-mass spectrometry (ESI-MS) (Mariner, PerkinElmer Life Sciences). Regarding the inhibitors, after removal of side chain protecting groups, final crude peptides were resuspended in diethyl ether to eliminate excess reagents and lyophilized. The effective concentration of dec-peptide-cmk was evaluated by mass ESI-MS.

Synthesis of Lassa GPC-derived Non-fluorogenic Peptides—The synthesis of the non-fluorogenic peptides ($GPC^{250-265}$ and GPC^{mut}, Fig. 3*C*) was performed using SPPS and N^{α}-*t*-butyloxycarbonyl (Boc) amino acids on Boc-Thr(Bzl)-PAM resin (NovaBiochem, La Jolla, CA, 0.34 mmol/g). After removal of the formyl protecting group (10% piperidine in DMF, 0 °C for 2 h), peptide cleavage and side chain deprotection were achieved using 12 ml of a mixture of 82% hydrofluoric acid, 9% thioanisole, and 9% dimethyl sulfoxide (Me_2SO) at −5 °C for 1 h. The crude products were purified by RP-HPLC on a semi-preparative Vydac C_{18} column (5 μm, 300 Å, 10 × 250 mm) in the above reported conditions. The peptides were assayed for purity (100%) by analytical RP-HPLC and their identity confirmed by ESI-MS.

Peptide Preparation—All lyophilized peptides were dissolved in H_2O except the 8-mer WT, dec-YISRRLL-cmk, and dec-ISRRLL-cmk that were dissolved in Me_2SO.

Source of Recombinant hSKI-1—Soluble human SKI-1, lacking the transmembrane domain and cytosolic tail (BTMD-SKI-1) and containing a C-terminal hexa-histidine tag was isolated from overnight media of HEK 293 cells stably expressing this BTMD-SKI-1, as described (6, 33). The presence of SKI-1 activity was measured with the 7-mer WT (optimal at pH 7.5), its ability to be inhibited with 300 μM 4-(2-aminoethyl)benzenesulfonyl fluoride (32), 10 mM EDTA, or 1 mM Zn^{2+} (25), and the absence of basic amino acid-specific furin-like cleavages tested with the pyroglutamic acid-RTKR-MCA (Pyr-RTKR-MCA, Peptide Institute Inc.) as described (34), were confirmed.

In Vitro Enzymatic Assays—Each reaction was carried out in a 100-μl buffer (25 mM Tris-HCl, 25 mM MES, and 1 mM $CaCl_2$ adjusted to pH 7.5) at 37 °C. The reactions contained 100 μM MCA peptide and 30 μl of hSKI-1 preparation. Enzymatic activity measurements with MCA-conjugated peptidyl substrates were performed by measuring the liberated 7-amino-4-methylcoumarin (AMC) with a Spectra MAX GEMINI EM microplate spectrofluorometer, Molecular Devices (λ_{ex}, 360 nm; λ_{em}, 460 nm). Enzymatic activity on non-fluorogenic peptidyl substrates were monitored by RP-HPLC under the following conditions: Varian analytical C_{18} (5 μM, 100 Å, 4.5 × 250 mm) column; flow, 1 ml/min, eluent A, 0.1% trifluroacetic acid/H_2O; eluent B, 0.1% trifluroacetic acid/CH_3CN; detector, 214 and 280 nm.

Determination of V_{max} and K_m Kinetic Parameters—For measurement of V_{max} and K_m kinetic parameters, hSKI-1 (30 μl) was incubated with increasing concentrations (20–200 μM) of each fluorogenic peptide in 100 μl of buffer in a 96-well microtiter plate at 37 °C under the above conditions. V_{max} and K_m values were estimated by Grafit 4.09. (Erithacus Software Ltd., Staines, United Kingdom). The software fits data to the Michaelis-Menten equation, where the rate is plotted as a function of the concentration of the substrate. Initial estimates are provided by use of linear fitting using the Scatchard rearrangement. Initial rates were evaluated for each peptide at different concentrations using the SOFTmaxPro 4.1 program based on the linear portion of the curve. We did not consider in the calculation the lag phase, which is probably due to the presence of inactive SKI-1 that might require time to be activated. In fact, the lag time is greatly reduced upon preincubation at 37 °C (not shown). We estimate that at least 5–10% of the fluorogenic peptide was digested within the analysis period. A similar phenomenon was also observed for the convertase PC1, where the lag phase could last up to 6 h (35).

In Vitro Inhibition of Succ-IYIRRLL-MCA Processing—Each reaction was carried out in a 100-μl buffer (25 mM Tris-HCl, 25 mM MES, and 1 mM $CaCl_2$ adjusted to pH 7.5) at 37 °C. The solutions, containing 30 μl of the hSKI-1 preparation and 5 μl of inhibitors at different concentrations (0–1.5 × 10^3 μM, dec-RRLL-cmk; 0–38 μM, dec-ISRRLL-cmk; 0–36 μM, dec-YISRRLL-cmk) were incubated 20 min at 37 °C before adding 50 μM Succ-IYISRRLL-MCA as substrate. Enzymatic activity measurements were performed by measuring the liberated AMC group with a Spectra MAX GEMINI EM microplate spectrofluorometer, Molecular Devices (λ_{ex}, 360 nm; λ_{em}, 460 nm).

Determination of in Vitro Inhibitor Constant IC_{50} Values—For measurements of IC_{50} values, hSKI-1 (30 μl) was incubated with increasing concentrations (0–1.5 × 10^5 nM, dec-RRLL-cmk; 0–38 μM, dec-ISRRLL-cmk; 0–36 μM, dec-YISRRLL-cmk) of each inhibitor in 100 μl of buffer, 50 μM Succ-IYISRRLL-MCA as substrate, in a 96-well microtiter plate at 37 °C under the above conditions. IC_{50} values were calculated by using GraFit version 4.09 software.

In Vitro Inhibition of Pyr-RTKR-MCA Processing—Each reaction was carried out in a 100-μl buffer (25 mM Tris-HCl and 1 mM $CaCl_2$, adjusted to pH 7.0 or 6.0) at 37 °C. The solutions, containing 1 μl of either concentrated human furin medium or 10 μl of mouse PC5 or human PACE4 preparations (36) and 5 μl of inhibitors at different concentrations (0–15 μM, dec-RRLL-cmk; 0–15 μM, dec-YISRRLL-cmk) were incubated 20 min at 37 °C before adding 50 μM Pyr-RTKR-MCA as substrate. Enzymatic activity measurements were performed by measuring the liberated AMC with a Spectra MAX GEMINI EM microplate spectrofluorometer, Molecular Devices (λ_{ex}, 360 nm; λ_{em}, 460 nm).

Nuclear Magnetic Resonance (NMR) Analysis—NMR experiments were carried out on a Varian Inova 500 MHz. NMR characterization was performed in trifluoroethanol (TFE)/H_2O, 90:10 (v/v) and 70:30 (v/v), at 298 K. Samples were prepared by dissolving weighted amounts of each peptide in [D_3]TFE (99% isotopic purity, Aldrich) and H_2O, for final concentrations of ~1.3 mM. Chemical shifts were referenced to

internal sodium 3-(trimethylsilyl)[2,2′,3,3′-d_4] propionate (TSP). Two-dimensional experiments, such as total correlation spectroscopy, nuclear Overhauser effect spectroscopy (NOESY), rotating frame Overhauser effect spectroscopy, and double quantum-filtered correlated spectroscopy were measured with standard pulse sequences (37, 38). According to Wüthrich (39), identification of amino acid spin systems was performed by comparison of total correlation spectroscopy and DQF-COSY, although sequential assignment was obtained by the analysis of NOESY spectra. NOE analysis was achieved by means of NOESY spectra, acquired with 200- and 300-ms mixing times. NOE intensities were evaluated by integration of cross-peaks from the 200-ms NOESY using NMRVIEW (40) software and then converted into inter-proton distances using the program CALIBA of the DYANA (41) package. Geminal protons, not stereospecifically assigned, were substituted by pseudo atoms (42).

SKI-1 substrates	P8	P6	P4	P2	P2′	P4′
(h) proSKI-1 site B	R	K	V	F	R	S
site B′	V	T	P	Q	R	K
site C	R	H	S	S	R	R
(h) SREBP-2	S	G	S	G	R	S
(h) SREBP-1	H	S	P	G	R	N
(h) ATF6	A	N	Q	R	R	H
(h) Luman	G	V	L	S	R	Q
(h) BBF2H7 (CREB3L2)	V	V	R	S	R	N
(m) OASIS (CREB3L1)	Q	M	P	S	R	S
(h) CREB-H	R	V	F	S	R	T
(h) CREB4	G	V	T	S	R	N
(h) BDNF	K	A	G	S	R	G
(r) Somatostatin	D	P	R	L	R	Q
Lassa (LAV)	I	Y	I	S	R	R
CCHFV	S	S	G	S	R	R
LCMV	K	F	L	T	R	R

SKI-1 substrates	P6	P4	P2	P2′	P4′
(h) proSKI-1 site B	K	V	F	Y	E
site B′	T	P	Q	F	S
site C	H	S	R	L	A
(h) SREBP-2	G	S	V	S	S
(h) SREBP-1	S	P	V	G	E
(h) ATF6	N	Q	L	G	S
(h) Luman	V	L	L	A	P
(h) BBF2H7 (CREB3L2)	V	R	L	I	E
(m) OASIS (CREB3L1)	M	P	L	F	D
(h) CREB-H	V	F	H	N	A
(h) CREB4	V	T	I	T	D
(h) BDNF	A	G	G	S	D
(r) Somatostatin	P	R	F	Q	L
Lassa (LAV)	Y	I	L	T	T
CCHFV	S	G	L	S	S
LCMV	F	T	L	T	T

FIGURE 1. **Amino acid sequences at the SKI-1/S1P cleavage site of mammalian and viral precursors.** The alignment shows the sequences between amino acid positions P4′ and P8 of the natural mammalian and viral substrates of SKI-1/S1P. The *arrows* indicate the cleavage site. The critical recognition amino acids Arg at P4 and hydrophobic amino acid at P2 are emphasized in *bold*.

Ex Vivo Inhibition of the SKI-1/S1P Processing of Pro-SREBP-2 and Pro-ATF6—For SREBP-2 analyses, CHO K1 cells were incubated overnight with various concentrations of decanoylated chloromethylketone inhibitors, namely the 7-mer-cmk (dec-YISRRLL-cmk, 0–110 μM), 6-mer-cmk (dec-ISRRLL-cmk, 0–110 μM), and commercial 4-mer-cmk (dec-RRLL-cmk; Bachem, 0–150 μM). Cell lysates were then analyzed for endogenous SREBP-2 or exogenously expressed ATF6 immunoreactivity by Western blots, as described (33). For ATF6 analyses the cells were first transiently transfected with ATF6 cDNA and then incubated the next day with the inhibitors.

Ex Vivo Inhibition of the Furin-like Processing of Pro-PDGF-A—On day 0, a stable PDGF-A-V5 construct in HEK 293 cells was plated on 35-mm plates in Dulbecco's modified Eagle's medium containing 100 units/ml gentamycin supplemented with 5% heat inactivated fetal calf serum. On day 1, cells were washed twice with 1× phosphate-buffered saline and serum-free medium was added along with varying concentrations of dec-YISRRLL-cmk (0–110 μM), dec-ISRRLL-cmk (0–110 μM), or dec-RRLL-cmk (0–150 μM), and incubated overnight. On day 3, medium was analyzed by running the samples on 12% SDS-PAGE and immunoblotted using V5-horseradish peroxidase antibody, 1:5000.

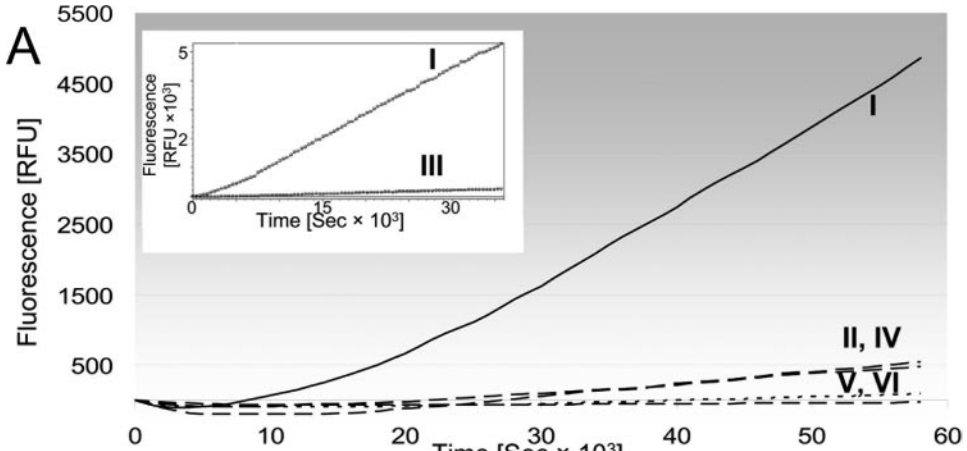

B

Peptide	Cleavage	Derivation
I. Succ-YISRRLL-MCA	+++	LAV
II. Succ- ISRRLL-MCA	+	LAV
III. Succ- RRLL-MCA	+	LAV
IV. Succ-SGSRRLL-MCA	+	CCHF
V. Succ-FLTRRLS-MCA	−	LCMV (WE)
VI. Succ-FFTRRLA-MCA	−	LCMV (Armostrong)

FIGURE 2. **SKI-1 activity on MCA-conjugated viral glycoprotein peptide substrates.** Fluorescence *versus* hydrolysis time of: *A*, Succ-YISRRLL-MCA (*I*) and Succ-ISRRLL-MCA (LAV-derived) (*II*), Succ-SGSRRLL-MCA (CCHFV-derived) (*IV*), and Succ-FLTRRLS-MCA (*V*) and Succ-FFTRRLA-MCA (LCMV Virus derived) (*VI*). *Inset*, comparison of the fluorescence released from Succ-YISRRLL-MCA (*I*) *versus* that of Succ-RRLL-MCA (*III*). *B*, summary of the cleavage preferences of the above peptides by SKI-1, +++, much better cleavage than +, and − meaning no cleavage.

RESULTS

Design and Evaluation of SKI-1 Fluorogenic Peptide Substrates—One of the major aims of the present study was to develop small MCA-containing fluorogenic substrates of SKI-1. Alignment of the recognition motifs of all known SKI-1 substrates revealed that except for the autocatalytic shedding sequence (KHQKLL ↓) (6), almost all sites contain an Arg at position P4 and hydrophobic residues at P2 with Leu and Val being most prevalent (exceptions include Ile for CREB4 and Phe for prosomatostatin) (Fig. 1). *In vitro* analysis showed that SKI-1 cleaves a 12-mer synthetic peptide (LWKHQKLL↓SIDL) derived from its shed site (6). However, when we analyzed at various pH values the processing of MCA-containing peptides mimicking this site, such

as the wild type Succ-WKHQKLL-MCA, and its P5 mutants Succ-WKRQKLL-MCA, Succ-WKKQKLL-MCA, or Succ-WKAQKLL-MCA, none were significantly processed (*not shown*). This suggested that for this substrate particularly, either extended P and/or P′ residues were important for SKI-1 recognition. Therefore, to test for potential *in vitro* SKI-1 substrates lacking P′ sites, we decided to synthesize a series of MCA-containing substrates with an Arg at P4 and a Leu at P2, based on the processing site of viral glycoproteins exhibiting potential SKI-1 recognition motifs, such as those found in LAV (24), CCHFV (28, 33), and LCMV (26) (Fig. 2*B*). The glycoprotein GPC of LAV was shown to be cleaved very well *in vitro* using a 14-mer quenched fluorogenic substrate (25). In the present study, analysis of the processing of these viral-derived peptides revealed that the order of SKI-1 cleavage preference is: 7-mer LAV GPC ≫ 6-mer LAV GPC ≈ 4-mer LAV GPC (Fig. 2*A*, *inset*) ≈ 7-mer CCHV glycoprotein (Fig. 2, *A* and *B*), whereas the chosen LCMV-derived substrates were not cleaved (Fig. 2, *A* and *B*). Because SKI-1 processing usually occurs in the medial Golgi where the pH is close to 6.4, we tested the cleavage of peptides IV, V, and VI (see Fig. 2*B*) at pH values of 7.5, 6.7, 6.3, and 6.0. Results showed that these peptides are not cleaved *in vitro* at acidic pH values (*not shown*), even though their parent glycoprotein precursors are likely to be cleaved *in vivo* in the Golgi. It is not excluded that *in vitro* cleavage of the latter peptides may require extended P or the presence of P′ residues, as it is the case of the LCMV *in vivo* processing (26).

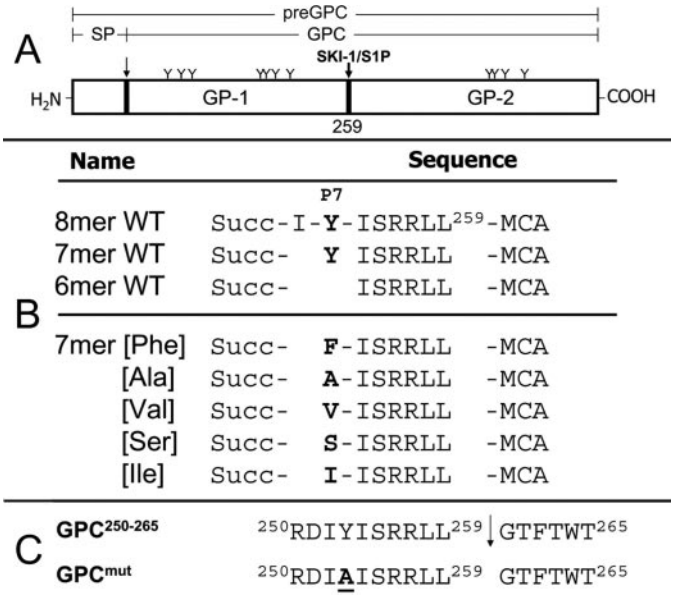

FIGURE 3. **Schematic representation of LAV GPC and synthetic peptides derived from the SKI-1 recognition site.** *A*, *SP* represents the signal peptide. *GP-1* and *GP-2* are the maturation products resulting from GPC cleavage (*arrow*) that occurs after recognition motif ^{256}RRLL^{259} by SKI-1. Y-shaped projections represent predicted *N*-linked glycosylation sites. Names and sequences of the wild type and point mutated fluorogenic (*B*) and non-fluorogenic (*C*) substrates derived from the GPC sequence.

The above results revealed that the cleavage rate of Lassa 6-mer GPC (Succ-ISRRLL-MCA) is comparable with that of a 7-mer peptide (Succ-SGSRRLL-MCA) mimicking the CCHFV glycoprotein processing site, but that the 7-mer GPC Lassa (Succ-YISRRLL-MCA) was a more than 14-fold better substrate than either of the above, even though all contain the common P5-P1 SRRLL sequence (Fig. 2). Thus, we hypothesized that Tyr at the P7 position within the GPC sequence of LAV plays a critical role. Accordingly, we synthesized MCA substrates with mutated P7 Tyr into Phe, Ile, Val, Ser, or Ala, as well as an 8-mer wild type sequence Succ-IYISRRLL-MCA (Fig. 3). Based on the optimal pH for the 7-mer peptide processing (Fig. 4, *inset*) and the absence of a [Ca^{2+}] effect on the SKI-1 activity from 0.5 to 20 mM (*not shown*), we chose to compare the SKI-1 cleavage of these peptides at pH 7.5 and 1 mM Ca^{2+}. The data revealed that the 8-mer is the best substrate for SKI-1, exhibiting a ~2.4-fold better V_{max}/K_m *versus* the 7-mer, whereas only the Phe mutant 7-mer is relatively well cleaved (Fig. 4, Table 1). Thus, within the context of the LAV GPC sequence only the aromatic amino acid Phe (also found at P7 in LCMV; Fig. 1) can somewhat replace Tyr, but not the other tested hydrophobic amino acids such as Val or Ile or even Ala or the hydroxyl-containing Ser. Thus, whereas Val occupies the P7 position in the cleavage sites of CREB-like and Luman, Ala in pro-brain-derived neurotropic factor and Ser in CCHFV and SREBP-1 (Fig. 1), these amino acids are not acceptable within the LAV GPC sequence. We conclude that the 8-mer and 7-mer wild type LAV GPC sequences represent the best MCA-containing SKI-1 substrates.

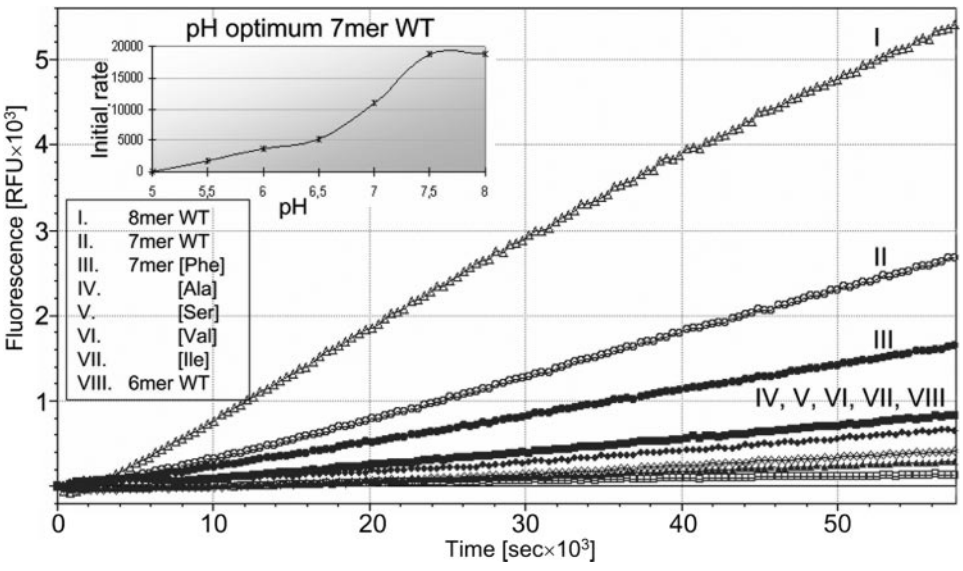

FIGURE 4. **SKI-1 activity on wild type and point mutated LAV GPC-derived MCA substrates.** Comparison of the AMC-released fluorescence *versus* time for the wild type and the P7 point mutated peptides (*I–VIII*) derived from the glycoprotein processing site of LAV. *Inset*, monitoring the SKI-1 activity on the 7-mer WT peptide at different pH values is reported. The higher initial rate was reached at pH 7.5.

Enzymatic Assays of Non-fluorogenic SKI-1 Peptide Substrates Derived from the LAV GPC Sequence—MCA peptides provide a highly sensitive approach for monitoring enzymatic cleavage C-terminal to an amino acid attached to the MCA moiety, as fluorescence is detected only when the AMC group is released. On the other hand, the analysis of the possible contribution of P′ residues to catalysis requires the use of a different approach, including quenched fluorogenic substrates (25) or non-derivatized peptides (6). Consequently, we synthesized two 16-mer non-fluorogenic substrates comprising six P′ positions mimicking the LAV glycoprotein processing site, namely $GPC^{250-265}$ and its Y253A P7 mutant (GPC^{mut}; Fig. 3). As shown by RP-HPLC analysis, the wild type $GPC^{250-265}$ peptide is much better processed over 16 h by SKI-1 as compared with the GPC^{mut} (Fig. 5). We estimated that 26% processing of $GPC^{250-265}$ occurred within 5 h, whereas a similar extent of cleavage is not achieved for GPC^{mut} even after a 16-h incubation. These data independently confirm that the P7 position in the LAV GPC sequence plays a critical role in substrate recognition.

NMR Analysis of the $GPC^{250-265}$ and GPC^{mut}—In an attempt to rationalize the importance of the P7 residue in the LAV GPC processing site, we determined the NMR structure of the wild type and mutant 16-mer peptides. Such an analysis was performed in 70:30, TFE/H_2O, and 90:30, TFE/H_2O. TFE is well known to favor solvent-shielded amide conformations, thus promoting ordered structures. It has been reported that local conformation of native proteins is usually better reproduced by the conformation assumed by corresponding fragments in solutions of TFE/H_2O (43, 44) than in pure water (45). However, as circular dichroism investigations performed at pH 7 have shown aperiodic structures for all the peptides (not shown), and as the enzymatic assays were performed in aqueous solutions, the real conformations adopted when the peptides interact with the enzyme remain speculative.

The NMR resulting proton chemical shifts $GPC^{250-265}$ and GPC^{mut} and the negative deviations >0.1 ppm point to a helical segment in the region from Ile^{253} to Leu^{259}. These findings are in agreement with a circular dichroism analysis of these peptides (not shown). The nuclear Overhauser effect (NOE) patterns confirm the possible occurrence of the helical structure in this region, as evidenced by the presence of diagnostic helical medium range effects of the type $\alpha N(i,i+3)$ and $\alpha\beta(i,i+3)$ in this area (39).

For the DG/Amber calculations a set of 116 experimental constraints from NOE data (81 intra-residual, 29 sequential, 6 medium range) was used for structure calculations of the peptide $GPC^{250-265}$ and 108 experimental constraints from NOE data (69 intra-residual, 34 sequential, 5 medium range) for GPC^{mut}. The best 10 structures for $GPC^{250-265}$ with residual restraint energy lower than −112 kcal/mol and for GPC^{mut} lower than −182 kcal/mol were selected to represent the solution structure of these peptides (Fig. 6*A*). For both peptides, a 3_{10} helix turn is found in the segment Ile^{254}–Arg^{257} (root mean square deviations ~ 0.50 ± 0.20 Å). A superimposition of the average solution conformations of $GPC^{250-265}$ (*black*) and GPC^{mut} (*gray*) is shown in Fig. 6*B*. These data suggest that the cleavage site follows a helical segment and that the presence of Ala instead of Tyr at P7 does not seem to perturb this secondary structure. However, even though the N-terminal segment, which includes the Y253A mutation, is quite flexible (Fig. 6*A*), the data suggest that the wild type and mutant conformations are not identical around Tyr^{253} *versus* Ala^{253} (*Y253*/*A253* in Fig. 6*B*). It is thus likely that

TABLE 1
Kinetic parameters of MCA-peptidyl SKI-1 substrates

Name	K_m	V_{max}	V_{max}/K_m
	μM	units × s^{-1}	units × 10^{-3} × s^{-1} × μM^{-1}
8-mer WT	14.8	0.155	10.5
7-mer WT	34.2	0.137	4.3
7-mer Phe	38.1	0.094	2.5
7-mer Ile	36.7	0.046	1.3
7-mer Ser	59.4	0.049	0.8
7-mer Ala	73.35	0.050	0.7
7-mer Val	137.8	0.050	0.4
6-mer WT	266.9	0.090	0.3

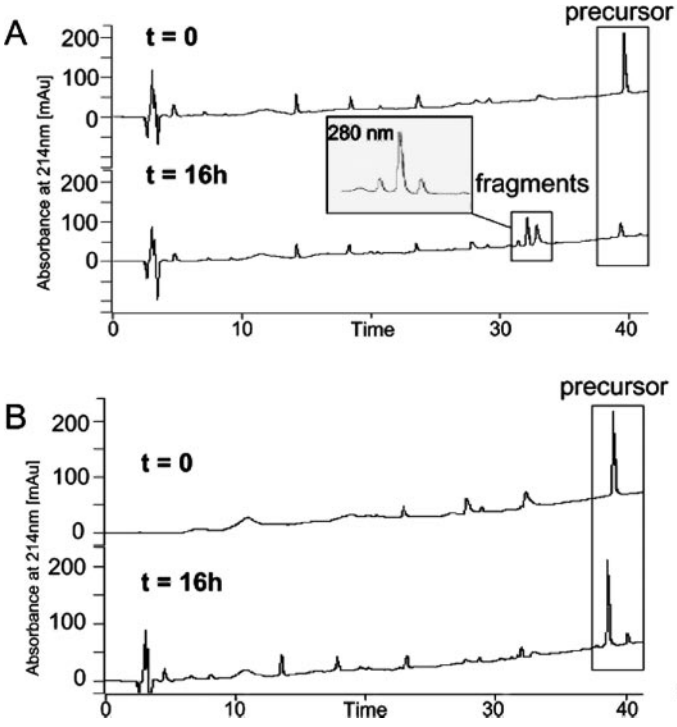

Digestion time [h]	% processing
0	0
3	16
5	26
7	31
16	77

$GPC^{250-265}$
^{250}RDIYISRRLLGTFTWT^{265}

Digestion time [h]	% processing
0	0
3	-
5	-
7	-
16	1

GPC^{mut}
^{250}RDIAISRRLLGTFTWT^{265}

FIGURE 5. **$GPC^{250-265}$ is efficiently processed by SKI-1, whereas GPC^{mut} is not.** The SKI-1 enzymatic cleavage of $GPC^{250-265}$ (*A*) and GPC^{mut} (*B*) was monitored by RP-HPLC at both 214 and 280 nm. Note that cleavage product GTFT**W**T^{265} can be identified as the peptide under the major peak at 280 nm. The % processing was estimated from the equation: (100 − % remaining precursor), and the precursor levels were evaluated by integrating the area of the corresponding peak.

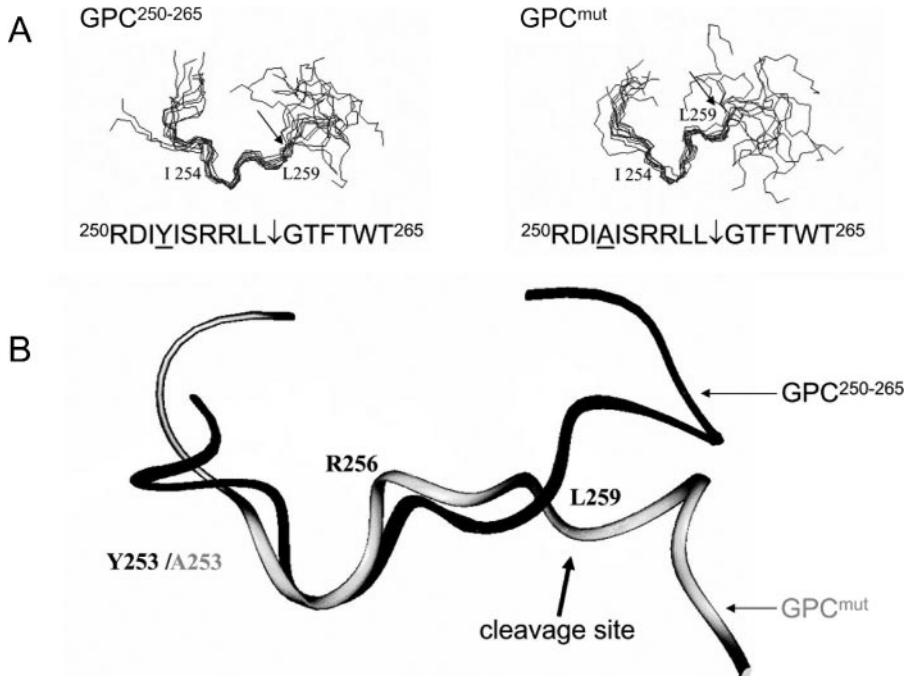

FIGURE 6. **NMR analyses of GPC$^{250-265}$ and GPC^{mut}.** *A*, superposition of the backbone from residue Ile^{254} to Leu^{259} of the best 10 structures after minimization with Amber for GPC$^{250-265}$ and GPC^{mut}, in TFE/H_2O, 70:30. *B*, backbone superposition of the molecular models (in TFE/H_2O, 70:30) for GPC$^{250-265}$ (*black ribbon*) and GPC^{mut} (*gray ribbon*) in segment Ile^{254} to Leu^{259}. Each structure represents the mean value of over 10 representative conformations after minimization with Amber.

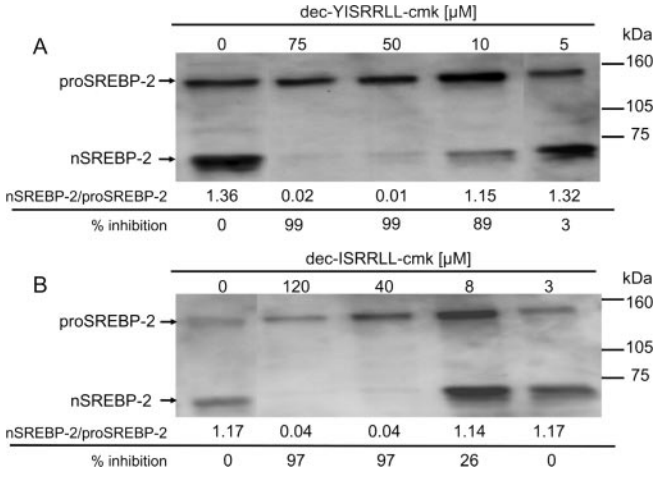

FIGURE 7. **Dec-YISRRLL-cmk and dec-ISRRLL-cmk are effective inhibitors of endogenous pro-SREBP-2 *ex vivo* processing.** CHO K1 cells were treated with medium containing delipidated serum (LPDS), 50 μM compactin, and 50 μM sodium mevalonate in the absence or presence of different concentrations of dec-YISRRLL-cmk (*A*) or dec-ISRRLL-cmk (*B*) for 18 h. Western blot analyses of the cell lysates was performed using a mouse monoclonal antibody directed against the NH_2-terminal domain of hamster SREBP-2. The *arrows* point to the migration position of the precursor pro-SREBP-2 and its mature nuclear form nSREBP-2. Molecular masses are given in kDa.

the observed preference of SKI-1 for phenylic structures at the P7 position of LAV GPC substrates may be better understood within the context of the enzyme-substrate complex than within that of the substrate alone.

Development of Potent Cell-permeable Peptidyl Chloromethylketone SKI-1 Inhibitors—The aim here was to develop potent cell-permeable, N-terminal decanoylated irreversible peptide inhibitors of SKI-1 activity containing a C-terminal Leu-cmk. On the basis of the above results, we compared the *ex vivo* inhibitory potential of an untested, yet commercially available, dec-RRLL-cmk to two other synthetic peptides made by us, namely the 6-mer dec-ISRRLL-cmk and 7-mer dec-YISRRLL-cmk (Figs. 7 and 8). The selected *ex vivo* SKI-1 precursor substrates were the membrane-bound transcription factors pro-SREBP-2 (46) and pro-ATF6 (17, 18), whose Golgi-associated cellular processing into their nuclear form nSREBP-2 and nATF6 can be inhibited by protein-based SKI-1 inhibitors (33). We first compared the inhibition of the processing of endogenous pro-SREBP-2 by the 6-mer *versus* 7-mer cmk-peptides (Fig. 7). The data showed that both peptides are potent *ex vivo* inhibitors of this SKI-1-generated cleavage with an estimated 50% inhibition at ~7 and ~20 μM for the 7-mer-cmk and 6-mer-cmk, respectively (Fig. 7). In another experiment we found that both 4-mer-cmk and 7-mer-cmk peptides are almost equipotent in inhibiting the processing of the overexpressed pro-ATF6 into nATF6 following ER stress induced by overnight tunicamycin treatment of CHO cells (17, 18, 33). We estimate that 50% inhibition occurs at $\leq$1 μM of either cmk-peptide (Fig. 8). Accordingly, we can conclude that the dec-4mer-cmk, dec-6mer-cmk, and dec-7mer-cmk cell-permeable SKI-1 inhibitors are almost equipotent *ex vivo*.

We next defined the selectivity of the above cmk-peptides for inhibition of SKI-1 *versus* other convertase-generated processing reactions. Accordingly, we opted to test the ability of the 7-mer cmk-peptide to inhibit processing of the precursor of the platelet-derived growth factor pro-PDGF-A into PDGF-A by furin-like basic amino acid-specific convertases (47), and to compare its potential inhibitory effect to that of the frequently used commercially available furin-like convertase inhibitor dec-RVKR-cmk (48). The data showed that in HEK 293 cells stably expressing pro-PDGF-A, the processing of this precursor by endogenous furin-like convertases is completely inhibited by ~3 μM dec-RVKR-cmk (Fig. 9*A*), whereas it would take >100 μM to inhibit less than 2% of this reaction by the 7-mer dec-YISRRLL-cmk (Fig. 9*B*) or 4-mer dec-RRLL-cmk (not shown).

Even though the above 4-, 6-, and 7-mer cmk-peptides were designed to be cell permeable through the attachment of an N-terminal decanoylated functionality, we were still interested in defining their *in vitro* inhibitory potency on processing of the 8-mer succ-IYISRRLL-MCA. Unexpectedly, the data shows 4-mer-cmk (IC_{50} ~ 9 nM) as a ~250-fold better inhibitor than either the 6- or 7-mer-cmk peptides (IC_{50} ~ 2,300 nM) (Fig. 10). This *in vitro* result could possibly be due to the presence of the highly hydrophobic decanoylated N-terminal moiety in these

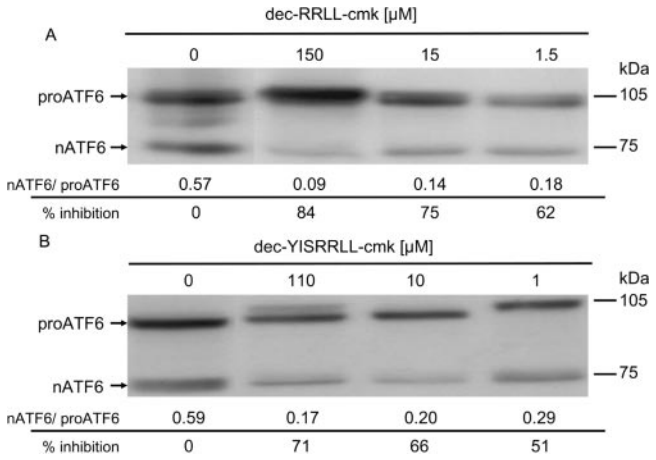

FIGURE 8. **Dec-YISRRLL-cmk and dec-RRLL-cmk are potent inhibitors of endogenous pro-ATF6 *ex vivo* processing.** Following transient transfection of CHO K1 cells with a cDNA coding for ATF6-FLAG, the cells were treated with varying concentrations of dec-RRLL-cmk (*A*) or dec-YISRRLL-cmk (*B*) in the presence of 2 μg/ml tunicamycin for 12 h. Western blot analyses of cell lysates was performed using an anti-FLAG M2 monoclonal antibody. The *arrows* point to the migration position of the precursor pro-ATF6 and its mature nuclear form nATF6. Molecular masses are given in kDa.

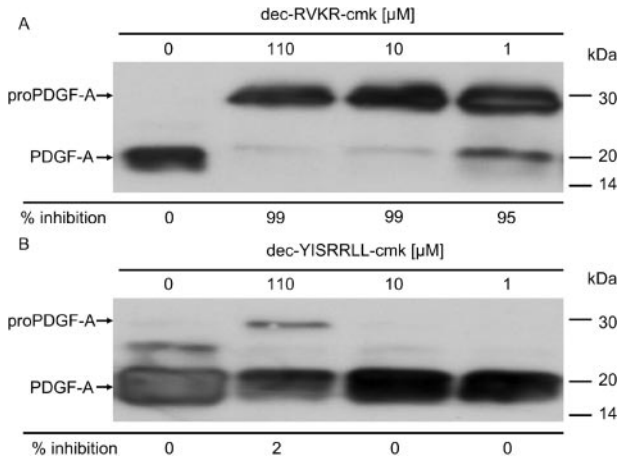

FIGURE 9. **Dec-YISRRLL-cmk is not an effective inhibitor of the *ex vivo* processing of pro-PDGF-A.** On day 1, HEK 293 cells, stably expressing the PDGF-A-V5 construct, were incubated overnight in serum-free medium with various concentrations of dec-YISRRLL-cmk (*B*) or dec-RVKR-cmk (*A*). On day 3, the media were fractionated on 12% SDS-PAGE and then analyzed by Western blot using a V5-horseradish peroxidase antibody. The *arrows* point to the migration position of the precursor pro-PDGF-A and its mature form PDGF-A. Molecular masses are given in kDa.

cmk-peptides. Accordingly, for the 6-mer-cmk and 7-mer-cmk it may be too hydrophobic and likely kinetically unfavorable, whereas for the 4-mer-cmk it may mimic the hydrophobic patch Ile-Tyr-Ile found at the P6 –P8 positions of the GPC LAV processing site. We can speculate that intracellularly, the decanoylated moiety is membrane-bound and hence may not exert such a negative effect (as compared with *in vitro*) on the inhibitory potency of the 7-mer-cmk and 6-mer-cmk peptides.

In a similar fashion we also compared the ability of the 4-mer-cmk and 7-mer-cmk peptides to inhibit *in vitro* furin processing of the pentapeptide pyr-RTKR-MCA. Interestingly, whereas these cmk-peptides do not inhibit either PC5 or PACE4, they are potent *in vitro* inhibitors of furin only at pH 7 (and pH 7.5, not shown), but much less at pH 6 (Table 2). Therefore, we conclude that whereas the designed cmk inhibitors are potent and relatively selective *ex vivo* inhibitors of SKI-1, they should be used with caution for *in vitro* reactions.

DISCUSSION

The main objectives of this study were centered around (i) the development of a simple fluorogenic substrate of SKI-1 that could be used in high throughput *in vitro* analysis of its activity, and (ii) use this information to design and synthesize a potent specific and cell-permeable SKI-1 peptidyl inhibitor.

For the first aim, we decided to test the ability of SKI-1 to cleave 7-mer MCA-containing peptides mimicking the glycoprotein recognition sequence of various hemorrhagic fever viruses. Unexpectedly, whereas intracellularly SKI-1 cleaves reasonably well the full-length glycoprotein of the LCMV-WE strain (26), it could not cleave *in vitro* the 7-mer-MCA peptides derived from either the WE or Armstrong strains (Fig. 2), suggesting that an extended sequence may be necessary for SKI-1 recognition. In contrast, the LAV GPC 7-mer sequence is well processed *in vitro*, much better than the 7-mer CCHFV mimic (Fig. 2), emphasizing the critical importance of the primary structure of the 7-mer substrate. The MCA-peptides derived from the GPCs of LAV and CCHFV only differ in their P7 and P6 positions, exhibiting Tyr-Ile and Gly-Ser residues, respectively (Fig. 2). This led us to investigate the critical residues in the LAV GPC sequence that makes it such a great substrate for SKI-1. Whereas the wild type 8-mer LAV GPC MCA-peptide is a 2-fold better substrate than the 7-mer, the latter is 14-fold better than the 6-mer (Fig. 4, Table 1). Interestingly, the 6-mer-MCA peptide derived from LAV GPC is processed by SKI-1 to the same extent as the 7-mer CCHFV peptide (Fig. 2, *A* and *B*). These data suggested that the P7 Tyr is much more critical than the P8 Ile for SKI-1 cleavage. Accordingly, to keep the substrate as short as possible while still retaining good cleavability and *in vitro* solubility, we tested whether other residues could replace the P7 Tyr in the 7-mer peptide by its mutation into various amino acids (Fig. 3*B*). The results showed that only Phe can partially replace the P7 Tyr, albeit with a loss of ~40% cleavability. All other mutants resulted in ≥70% loss of SKI-1 cleavability (Fig. 4, Table 1), emphasizing the importance of the P7 phenylic group for optimal SKI-1 recognition. Independently, we confirmed the critical importance of the P7 Tyr within the context of the LAV GPC sequence by analyzing the *in vitro* processing of a 16-mer peptide mimicking the wild type sequence from P6′ to P10 (Figs. 3*C* and 5*A*) and that of a Y253A mutant (Figs. 3*C* and 5*B*). In agreement with the above data, a similar observation of the critical presence of a phenylic group at P7 was also observed *ex vivo* for the cleavage of the glycoprotein of LCMV, because replacement of the P7 Phe (Fig. 1) by Ala resulted in an almost absence of SKI-1 processing (26).

Whereas the importance of the P7 Tyr residue was deduced from MCA substrates, the absence of cleavage by SKI-1 of the 16-mer Y253A mutant may conceivably be due to additional structural features of the peptide. Preliminary circular dichroism analysis in aqueous solution of the non-fluorogenic 16-mer wild type and its Y253A mutant did not reveal significant conformational differences between them (not shown). We next opted for the comparison of the NMR structure of these 16-mer

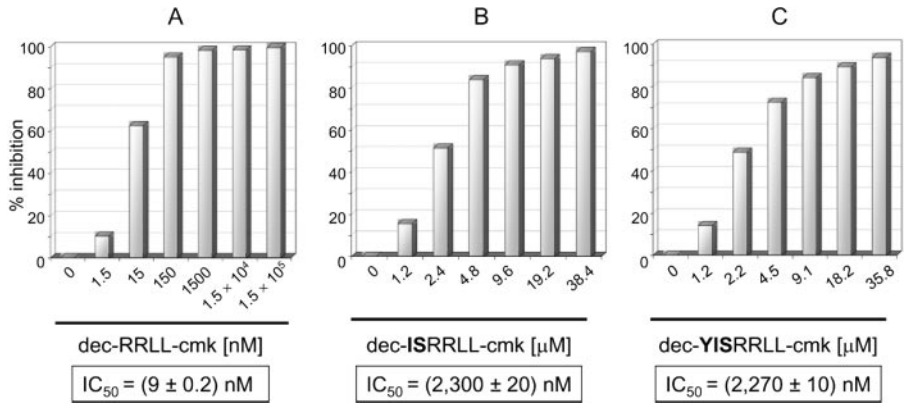

FIGURE 10. **Dec-RRLL-cmk, dec-ISRRLL-cmk, and dec-YISRRLL-cmk are effective inhibitors of Succ-IYISRRLL-MCA *in vitro* processing by SKI-1.** Concentration dependent inhibition of Succ-IYISRRLL-MCA *in vitro* SKI-1 mediated processing by dec-RRLL-cmk (*A*), dec-ISRRLL-cmk (*B*), and dec-YISRRLL-cmk (*C*). All inhibitory constants (IC_{50}) were evaluated with 50 μM substrate using GraFit version 4.09 as described under "Experimental Procedures."

TABLE 2

***In vitro* inhibition of the processing of Pyr-RTKR-MCA by PC-like enzymes**

Each reaction was carried out in a 100-μl, pH 7.0 or 6.0, buffer at 37 °C in the presence of different concentrations of dec-YISRRLL-cmk or dec-RRLL-cmk. The % inhibition was evaluated from initial rate values.

	% Inhibition			
	Furin (pH 6)	Furin (pH 7)	PC5 (pH 7)	PACE4 (pH 7)
Dec-YISRRLL-cmk				
0	0	0	0	0
10^{-9}	0	47		
10^{-8}	0	62		
10^{-7}	0	51		
10^{-6}	0	42		
10^{-5}	67	75	2	0
Dec-RRLL-cmk				
0	0	0	0	0
1.5×10^{-9}	0	61		
1.5×10^{-8}	0	54		
1.5×10^{-7}	0	49		
1.5×10^{-6}	0	44		
1.5×10^{-5}	0	63	0	0

peptides. The data revealed that both peptides exhibit a helical structure from Ile^{254} to Arg^{257}, and do not significantly differ from each other at the SKI-1 cleavage site $RRLL^{259}\downarrow$. However, the Y253A mutation may partially affect the solution structure of the peptide at the N-terminal segment preceding Ile^{254} (Fig. 6). We conclude that the rationale behind the observed large difference in SKI-1 cleavability of these 16-mer peptides (Fig. 5) does not reside in the secondary structure of the free substrate, but that likely the P7 Tyr plays a critical role in binding the substrate to the catalytic pocket of SKI-1.

Because we do not have an active site titrant of SKI-1, it is not possible presently to convert our V_{max} data into k_{cat} with confidence. The same applied to our previously published quenched fluorogenic substrates (25). Because the kinetics are really different between the quenched fluorogenic substrates and the MCA-containing ones proposed in this work (not shown), it is presently difficult to directly compare the two types of substrates. Nevertheless, we tested both types of substrates and observed that after a 2-h incubation both assays are similarly sensitive. Finally, the choice of the MCA-containing substrates was to narrow down the selectivity of the substrate to SKI-1, whereas the longer quenched fluorogenic substrates could be cleaved by other enzymes.

Our next aim was to design irreversible peptide inhibitors of SKI-1 based on the results obtained from MCA-peptide substrate studies and incorporating a C-terminal chloromethylketone reactive moiety. Furthermore, because we aimed to obtain cell-permeable inhibitors for *ex vivo* studies we introduced a hydrophobic decanoyl group at the N terminus of the designed peptides. Indeed, results from other studies on furin inhibitors revealed the critical importance of the addition of an N-terminal decanoyl group for cellular permeability of cmk-containing peptide inhibitors (49). On the basis of the above results we designed a decanoylated 7-mer-cmk peptide mimicking the LAV GPC sequence. To test the importance of the peptide length for cellular permeability and inhibition of SKI-1, we also compared *ex vivo* (Figs. 7 and 8) and *in vitro* (Fig. 10) inhibitory properties of dec-7mer-cmk to that of either a 1-amino acid shorter (dec-6mer-cmk) or 3-amino acid shorter, commercially available, dec-4mer-cmk. Unexpectedly, and in contrast to the LAV-GPC-derived MCA-substrate results (Table 1), we observed that the dec-6mer-cmk peptide was almost equipotent to the dec-7mer-cmk in inhibiting cellular processing of pro-SREBP-2 (Fig. 7). Furthermore, the dec-4mer-cmk peptide was equipotent to dec-7mer-cmk in inhibiting the cellular pro-ATF6 processing (Fig. 8). However, it must be mentioned that, whereas the LAV GPC sequence is so far the best substrate of SKI-1, peptides derived from either pro-ATF6 or pro-SREBP-2 turned out to be much poorer SKI-1 substrates (25). In addition, different from the succinyl-MCA substrates, the inhibitors used contain an N-terminal decanoyl group, which may influence their conformation upon membrane attachment and/or binding to the catalytic pocket of SKI-1. This is especially relevant in view of the observed poor cleavability of the 4-mer succ-RRLL-MCA (Fig. 2*A*, *inset*) and the importance of the hydrophobic residues Ile-Tyr-Ile at the P6 to P8 positions in the LAV GPC sequence (Figs. 3*B* and 4). We can conclude that dec-7mer-cmk, dec-6mer-cmk, and 4mer-cmk peptides are potent SKI-1 *ex vivo* inhibitors.

We next addressed the issue of selectivity of these *ex vivo* SKI-1 inhibitors and whether they could inhibit other convertases such as the basic amino acid-specific furin-like proteinases (2). This was especially relevant, because we recently observed that the *RXXR* motif is not always indicative of a furin-like recognition sequence, as the motif *RXLR* was also recognized by SKI-1 in both Luman (20) and a modified PDGF-A sequence (47). For this purpose we used a cell-based assay monitoring the processing of pro-PDGF-A into PDGF-A through cleavage by furin-like enzymes at the $RRKR^{86}\downarrow$ sequence (47), a process inhibitable by dec-RVKR-cmk (Fig. 9*A*). The data revealed that at concentrations $\leq$100 μM dec-7mer-cmk, which effectively inhibit SKI-1 activity *ex vivo* (Figs. 7 and 8), no sig-

nificant inhibition of pro-PDGF-A cleavage was observed (Fig. 9*B*). Note that at 110 μM dec-YISRRLL-cmk ~2% inhibition of pro-PDGF-A *ex vivo* processing was observed (Fig. 9*B*). The fact that furin prefers basic amino acid containing substrates with a Leu at P2′ and the presence of a Leu at P1′ prevents cleavage by this enzyme (2, 50), suggests that a peptide that contains all these characteristics, *e.g.* RRLL found in all our dec-peptide-cmks, could conceivably inhibit furin. Thus, we can conclude that when used at concentrations ≤100 μM, the dec-7mer-cmk is relatively specific for SKI-1 inhibition *ex vivo*.

Because we did not observe toxicity of the synthesized dec-RRLL-cmk on HEK 293 and CHO K1 cells, we collaborated with a group in the Center of Disease Control (Atlanta, GA) to test this inhibitor on live Lassa virus. Unfortunately, this compound was found to be toxic to Vero cells and cannot be used on this cell line, which is the model cell line used in Lassa virus infections.

Even though the cmk-peptides were designed to work in cells, we also tested their *in vitro* inhibitory potency and selectivity (Figs. 10, Table 2). The data revealed that all of them are effective inhibitors of the *in vitro* SKI-1 cleavage of a succinyl-8mer-MCA peptide derived from LAV-GPC, especially the dec-RRLL-cmk (IC_{50} ~ 9 nM). The high *in vitro* potency of the latter as compared with the 7-mer-cmk and 6-mer-cmk (IC_{50} ~ 2,300 nM) may in part be due to the presence of a common N-terminal decanoyl group added to an already very hydrophobic sequence within the latter two peptides, hence decreasing their solubility and/or increasing their tendency to form micelles in aqueous buffers. For comparison, the estimated *in vitro* IC_{50} of dec-RVKR-cmk for furin is ~2 nM (51). We therefore tested the *in vitro* inhibitory selectivity of dec-4mer-cmk and dec-7mer-cmk on the constitutively secreted convertases (2) furin at pH 7 and 6 (because processing of both pro-SREBP-2 and pro-ATF6 occurs in the medial Golgi with an intraluminal acidic pH), and PACE4/PC5A at pH 7. The data revealed that furin is not inhibited at pH 6 (Table 2), in agreement with the *ex vivo* data that gauged the activity of furin on pro-PDGF-A in the *trans* Golgi network (Fig. 9*B*) (47, 52). On the other hand, only furin is inhibited by both peptides at pH 7, whereas under the same conditions the activities of PC5A and PACE4 are not affected (Table 2). As mentioned above, an RRLL sequence could potentially inhibit furin, but because both PC5A and PACE4 can process peptides with P1′ Leu (53, 54) the latter convertases are not expected to be inhibited by this sequence. We can discard the possibility that the observed different inhibitory potential of the cmk-peptides on furin at pH 6 and 7 is due to the degradation of the cmk-peptides, because their levels did not significantly change upon incubation at either pH, as verified by mass spectrometry (not shown). The sizes of the inhibitor dec-RRLL-cmk and the substrate pyr-RTKR-MCA are too small to assume a rigid conformation in solution. However, because the reported crystal structure of furin was obtained at pH 6.0 (55), it is a matter of speculation whether the inhibition of furin at pH 7 by the cmk-peptides may be due to a different conformation of the enzyme at acidic *versus* neutral pH values. Along the same reasoning, it was recently demonstrated that the serpin α1-PDX and some of its mutants inhibit furin better at pH 7 than at pH 6 (56). If so, this may be an interesting avenue to pursue, as a number of proteins of mammalian, bacterial, and viral origin are processed by furin at the cell surface (52).

In conclusion, the data presented here provide a new framework for the development of potent cell-permeable SKI-1 inhibitors containing the central RRLL minimal core. Modifications of this structure as well as the addition of other inhibitory functionalities (57) may lead to specific and pharmacologically useful compounds to control SKI-1 activity *in vivo*. The availability of the proposed small MCA substrates should also help in following the *in vitro* activity of this enzyme under various physiological conditions.

Acknowledgments—We are indebted to Josée Hamelin, Mikhail Ponamarev, and Annik Prat for constant and precious advice and help. We gratefully acknowledge the precious help of Martin Vincent and Eric Bergeron on experiments using Lassa virus in Biosafety lab 4 (CDC, Atlanta, GA). The secretarial assistance of Brigitte Mary is greatly appreciated.

REFERENCES

1. Puente, X. S., Sanchez, L. M., Overall, C. M., and Lopez-Otin, C. (2003) *Nat. Rev. Genet.* **4,** 544–558
2. Seidah, N. G., and Chretien, M. (1999) *Brain Res.* **848,** 45–62
3. Seidah, N. G., and Prat, A. (2002) *Essays Biochem.* **38,** 79–94
4. Seidah, N. G., Benjannet, S., Wickham, L., Marcinkiewicz, J., Jasmin, S. B., Stifani, S., Basak, A., Prat, A., and Chretien, M. (2003) *Proc. Natl. Acad. Sci. U. S. A.* **100,** 928–933
5. Toure, B. B., Munzer, J. S., Basak, A., Benjannet, S., Rochemont, J., Lazure, C., Chretien, M., and Seidah, N. G. (2000) *J. Biol. Chem.* **275,** 2349–2358
6. Elagoz, A., Benjannet, S., Mammarbassi, A., Wickham, L., and Seidah, N. G. (2002) *J. Biol. Chem.* **277,** 11265–11275
7. Cheng, D., Espenshade, P. J., Slaughter, C. A., Jaen, J. C., Brown, M. S., and Goldstein, J. L. (1999) *J. Biol. Chem.* **274,** 22805–22812
8. Espenshade, P. J., Cheng, D., Goldstein, J. L., and Brown, M. S. (1999) *J. Biol. Chem.* **274,** 22795–22804
9. Benjannet, S., Rhainds, D., Essalmani, R., Mayne, J., Wickham, L., Jin, W., Asselin, M. C., Hamelin, J., Varret, M., Allard, D., Trillard, M., Abifadel, M., Tebon, A., Attie, A. D., Rader, D. J., Boileau, C., Brissette, L., Chretien, M., Prat, A., and Seidah, N. G. (2004) *J. Biol. Chem.* **279,** 48865–48875
10. Seidah, N. G., Mowla, S. J., Hamelin, J., Mamarbachi, A. M., Benjannet, S., Toure, B. B., Basak, A., Munzer, J. S., Marcinkiewicz, J., Zhong, M., Barale, J. C., Lazure, C., Murphy, R. A., Chretien, M., and Marcinkiewicz, M. (1999) *Proc. Natl. Acad. Sci. U. S. A.* **96,** 1321–1326
11. Sakai, J., Rawson, R. B., Espenshade, P. J., Cheng, D., Seegmiller, A. C., Goldstein, J. L., and Brown, M. S. (1998) *Mol. Cell* **2,** 505–514
12. Brown, M. S., and Goldstein, J. L. (1999) *Proc. Natl. Acad. Sci. U. S. A.* **96,** 11041–11048
13. Rawson, R. B., Zelenski, N. G., Nijhawan, D., Ye, J., Sakai, J., Hasan, M. T., Chang, T. Y., Brown, M. S., and Goldstein, J. L. (1997) *Mol. Cell* **1,** 47–57
14. Yang, T., Espenshade, P. J., Wright, M. E., Yabe, D., Gong, Y., Aebersold, R., Goldstein, J. L., and Brown, M. S. (2002) *Cell* **110,** 489–500
15. Rawson, R. B. (2003) *Biochem. Soc. Symp.* **70,** 221–231
16. Kaufman, R. J. (2002) *J. Clin. Investig.* **110,** 1389–1398
17. Haze, K., Yoshida, H., Yanagi, H., Yura, T., and Mori, K. (1999) *Mol. Biol. Cell* **10,** 3787–3799
18. Ye, J., Rawson, R. B., Komuro, R., Chen, X., Dave, U. P., Prywes, R., Brown, M. S., and Goldstein, J. L. (2000) *Mol. Cell* **6,** 1355–1364
19. Shen, J., Chen, X., Hendershot, L., and Prywes, R. (2002) *Dev. Cell* **3,** 99–111
20. Raggo, C., Rapin, N., Stirling, J., Gobeil, P., Smith-Windsor, E., O'Hare, P., and Misra, V. (2002) *Mol. Cell. Biol.* **22,** 5639–5649
21. Stirling, J., and O'Hare, P. (2006) *Mol. Biol. Cell* **17,** 413–426
22. Mouchantaf, R., Watt, H. L., Sulea, T., Seidah, N. G., Alturaihi, H., Patel,

Y. C., and Kumar, U. (2004) *Regul. Pept.* **120,** 133–140
23. Schlombs, K., Wagner, T., and Scheel, J. (2003) *Proc. Natl. Acad. Sci. U. S. A.* **100,** 14024–14029
24. Lenz, O., ter Meulen, J., Klenk, H. D., Seidah, N. G., and Garten, W. (2001) *Proc. Natl. Acad. Sci. U. S. A.* **98,** 12701–12705
25. Basak, A., Chretien, M., and Seidah, N. G. (2002) *FEBS Lett.* **514,** 333–339
26. Beyer, W. R., Popplau, D., Garten, W., Von Laer, D., and Lenz, O. (2003) *J. Virol.* **77,** 2866–2872
27. Kunz, S., Edelmann, K. H., de la Torre, J. C., Gorney, R., and Oldstone, M. B. (2003) *Virology* **314,** 168–178
28. Vincent, M. J., Sanchez, A. J., Erickson, B. R., Basak, A., Chretien, M., Seidah, N. G., and Nichol, S. T. (2003) *J. Virol.* **77,** 8640–8649
29. Johanning, K., Juliano, M. A., Juliano, L., Lazure, C., Lamango, N. S., Steiner, D. F., and Lindberg, I. (1998) *J. Biol. Chem.* **273,** 22672–22680
30. Ha, T. (2001) *Methods* **25,** 78–86
31. Basak, A., Zhong, M., Munzer, J. S., Chretien, M., and Seidah, N. G. (2001) *Biochem. J.* **353,** 537–545
32. Okada, T., Haze, K., Nadanaka, S., Yoshida, H., Seidah, N. G., Hirano, Y., Sato, R., Negishi, M., and Mori, K. (2003) *J. Biol. Chem.* **278,** 31024–31032
33. Pullikotil, P., Vincent, M., Nichol, S. T., and Seidah, N. G. (2004) *J. Biol. Chem.* **279,** 17338–17347
34. Zhong, M., Munzer, J. S., Basak, A., Benjannet, S., Mowla, S. J., Decroly, E., Chretien, M., and Seidah, N. G. (1999) *J. Biol. Chem.* **274,** 33913–33920
35. Rabah, N., Gauthier, D., Wilkes, B. C., Gauthier, D. J., and Lazure, C. (2006) *J. Biol. Chem.* **281,** 7556–7567
36. Decroly, E., Wouters, S., Di Bello, C., Lazure, C., Ruysschaert, J. M., and Seidah, N. G. (1996) *J. Biol. Chem.* **271,** 30442–30450
37. Bax, A., and Davis, D. G. (1985) *J. Magn. Reson.* **63,** 207–213
38. Jeener, J., Meier, B. H., Bachmann, P., and Ernst, R. R. (1979) *J. Chem. Phys.* **71,** 4546–4553
39. Wüthrich, K. (1986) *NMR of Proteins and Nucleic Acids*, J. Wiley & Sons, New York
40. Johnson, B. A., and Blevins, R. A. (1994) *J. Biomol. NMR* **4,** 603–614
41. Guntert, P., Mumenthaler, C., and Wuthrich, K. (1997) *J. Mol. Biol.* **273,** 283–298
42. Wuthrich, K., Billeter, M., and Braun, W. (1983) *J. Mol. Biol.* **169,** 949–961
43. Jimenez, M. A., Bruix, M., Gonzalez, C., Blanco, F. J., Nieto, J. L., Herranz, J., and Rico, M. (1993) *Eur. J. Biochem.* **211,** 569–581
44. Reymond, M. T., Huo, S., Duggan, B., Wright, P. E., and Dyson, H. J. (1997) *Biochemistry* **36,** 5234–5244
45. Callihan, D. E., and Logan, T. M. (1999) *J. Mol. Biol.* **285,** 2161–2175
46. Brown, M. S., and Goldstein, J. L. (1997) *Cell* **89,** 331–340
47. Siegfried, G., Khatib, A. M., Benjannet, S., Chretien, M., and Seidah, N. G. (2003) *Cancer Res.* **63,** 1458–1463
48. Bergeron, E., Vincent, M. J., Wickham, L., Hamelin, J., Basak, A., Nichol, S. T., Chretien, M., and Seidah, N. G. (2005) *Biochem. Biophys. Res. Commun.* **326,** 554–563
49. Garten, W., Hallenberger, S., Ortmann, D., Schafer, W., Vey, M., Angliker, H., Shaw, E., and Klenk, H. D. (1994) *Biochimie* (*Paris*) **76,** 217–225
50. Nakayama, K. (1997) *Biochem. J.* **327,** 625–635
51. Jean, F., Stella, K., Thomas, L., Liu, G., Xiang, Y., Reason, A. J., and Thomas, G. (1998) *Proc. Natl. Acad. Sci. U. S. A.* **95,** 7293–7298
52. Thomas, G. (2002) *Nat. Rev. Mol. Cell Biol.* **3,** 753–766
53. Mercure, C., Jutras, I., Day, R., Seidah, N. G., and Reudelhuber, T. L. (1996) *Hypertension* **28,** 840–846
54. Basak, A., Koch, P., Dupelle, M., Fricker, L. D., Devi, L. A., Chretien, M., and Seidah, N. G. (2001) *J. Biol. Chem.* **276,** 32720–32728
55. Henrich, S., Cameron, A., Bourenkov, G. P., Kiefersauer, R., Huber, R., Lindberg, I., Bode, W., and Than, M. E. (2003) *Nat. Struct. Biol.* **10,** 520–526
56. Dufour, E. K., Desilets, A., Longpre, J. M., and Leduc, R. (2005) *Protein Sci.* **14,** 303–315
57. Basak, A. (2005) *J. Mol. Med.* **83,** 844–855